J Mater Sci: Mater Electron (2013) 24:2944–2949
DOI 10.1007/s10854-013-1195-1

Effect of CuO addition on the microstructure and electrical properties of SnO_2-based varistor

Guangliang Hu · Jianfeng Zhu · Haibo Yang · Fen Wang

Received: 11 January 2013 / Accepted: 19 March 2013 / Published online: 27 March 2013

Abstract The effect of CuO addition on the properties of (Co, Nb, Cr)-doped SnO_2 varistors were investigated. The samples with different CuO concentrations were fabricated by the conventional ceramic method and sintered at 1,200, 1,250, 1,300 and 1,350 °C for 2 h. It is found that the nonlinear coefficient presents a peak value at 0.2 mol % CuO addition. The leakage current density decreases with increasing CuO from 0 to 0.2 mol %, and then increases when the concentration of CuO is above 0.2 mol %. The breakdown electrical field decreases from 356 to 248 V/mm with increasing CuO from 0 to 0.6 mol %. The optimal samples obtained by doping CuO with 0.2 mol % and sintered at 1,300 °C have the highest nonlinear coefficient value of 31 and the lowest leakage current density of 2 $\mu A/cm^2$.

1 Introduction

The rutile crystalline structural SnO_2 is an n-type semiconductor with many interesting electronic properties. In the past, it is widely used in gas sensors and wet sensors. However, since it is first studied as varistors by the group of Pianaro, a great number of papers on the new SnO_2-based varistors have been published [1–4]. Compared with the commercial ZnO varistors, it has good thermal conductivity and high temperature resistance. The main characteristic of this new varistor system is its simple microstructure, which has only one phase with X-ray precision. The single-phase microstructure of SnO_2 based varistors maybe resolve the problem of the degradation of the commercial ZnO–Bi_2O_3 based varistors.

In the past decades, many dopants have been studied, such as ZnO, CoO, MnO, Nb_2O_5, CuO, Ta_2O_5, Cr_2O_3, Al_2O_3 [5–13]. And the effects of these dopants are different in SnO_2-based varistor. ZnO, CoO, MnO have significant role to improve the density, Nb_2O_5 and Ta_2O_5 mainly improve the conductivity, and Cr_2O_3 and Al_2O_3 mainly improve current–voltage characteristic of SnO_2-based ceramics. From the recent publications, CoO, Nb_2O_3 and Cr_2O_3 doped SnO_2-based varistors show the excellent nonlinearity and high density [4, 14–17].

In the previous works [18, 19], the effects of CuO on the grain size, density, nonlinearity, and dielectric property of the SnO_2–Ni_2O_3–Nb_2O_5 and SnO_2–Co_2O_3–Ta_2O_5 varistors were investigated. In this work, the effects of CuO addition and sintering temperature on the microstructure and electrical properties of the Co_2O_3–Nb_2O_3–Cr_2O_3 doped SnO_2 varistors were investigated in detail. It is found that CuO addition and sintering temperature could evidently adjust the microstructure, and as a result, the breakdown electrical field decreases, the nonlinearity improves and the leakage current decreases.

2 Experimental

Five raw materials of analytic level, SnO_2 (99.8 %), Co_2O_3 (99 %), Nb_2O_5 (99.5 %), CuO (99 %) and Cr_2O_3 (99 %), were used to prepare the SnO_2 based varistors. The varistors were fabricated by a conventional electrical ceramics

G. Hu (✉) · J. Zhu · H. Yang · F. Wang
Key Laboratory of Auxiliary Chemistry and Technology for Chemical Industry, Ministry of Education, Shaanxi University of Science and Technology, Xi'an 710021, Shaanxi, China
e-mail: huguangliang@126.com

J. Zhu
e-mail: zhujf@sust.edu.cn

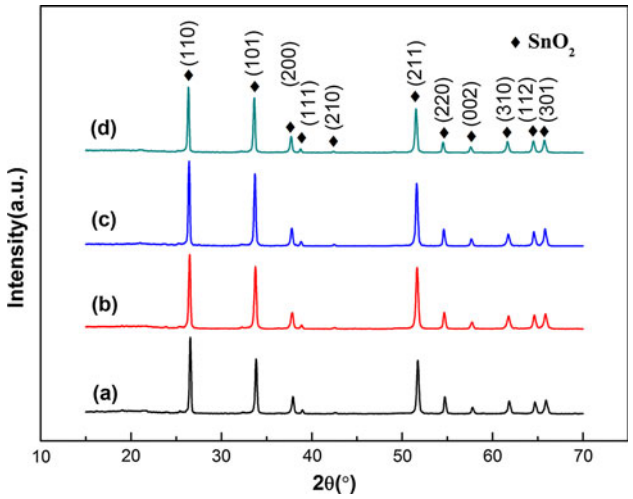

Fig. 1 XRD patterns of the SnO_2 based varistors doped with different amount of CuO at 1,300 °C: (*a*) without CuO; (*b*) 0.1 mol %; (*c*) 0.2 mol %; (*d*) 0.6 mol %

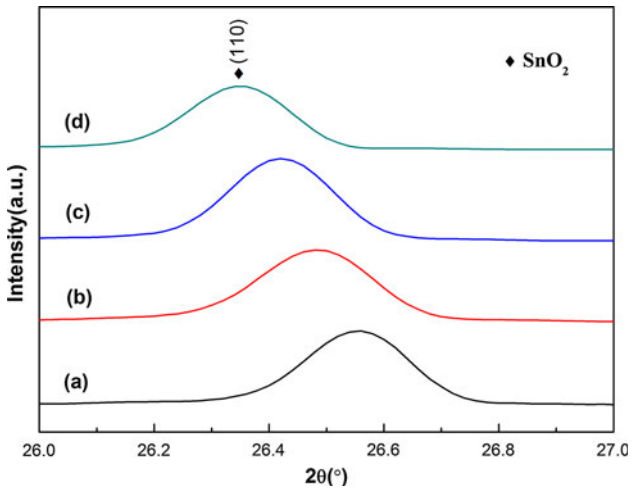

Fig. 2 The shifting of SnO_2 diffraction peaks with different amount of CuO at 1,300 °C

processing method. The compositions in molar ratios were (98.2 − X) % SnO_2 + 0.75 % Co_2O_3 + 0.05 % Nb_2O_5 + 0.05 % Cr_2O_3 + X % CuO, with X = 0.0, 0.1, 0.2, 0.4 and 0.6 mol %. The mixtures of raw materials were milled in nylon kettle for 4 h at 800 r/min with ZrO_2 balls and distilled water, the ratio of balls to the mixed powders and water was 2:1:1. Then as milled slurry was dried, mixed with 0.8 wt % of PVA binder and pressed into pellets (10.00 mm × 1.32 mm) by uniaxial pressing (2.5 MPa). After burning out the PVA binder at 650 °C for 2 h, the pellets were respectively sintered at 1,200, 1,250, 1,300, and 1,350 °C for 2 h, and then cooled to the room temperature at a rate of 5 °C/min.

The microstructures of the surfaces were analyzed by scanning electron microscopy (SEM, Model JSM-5610LV, JEOL), and the phase composition was determined by X-ray powder diffraction (XRD). The grain sizes (d) were calculated by microstructure linear analysis [20]. The sintered density (ρ) of ceramics was measured by the Archimedes method in distilled water. For the electrical measurements, silver electrodes (0.5 cm^2) were made on both surfaces of the sintered pellets, after which the pellets were heat-treated at 600 °C for 2 h. The I–V characteristics were measured by using a DC parameter instrument for varistors (Model CJ1001). The voltage gradient (V_{1mA}) was determined at a current of 1 mA and nonlinear coefficient (α) was obtained from the equation of $\alpha = 1/\lg(V_{1mA}/V_{0.1mA})$. The leakage current ($I_L$) was measured at $0.75V_{1mA}$.

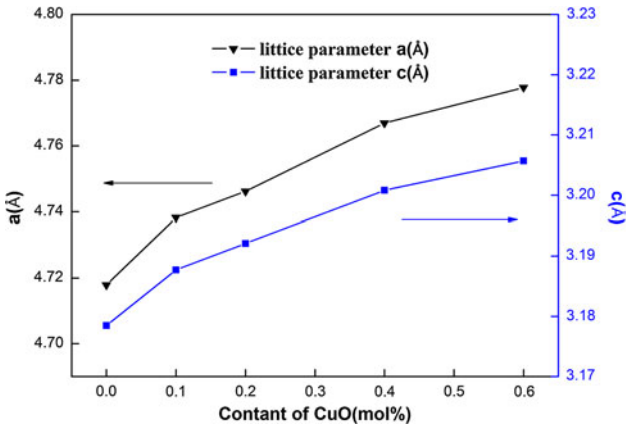

Fig. 3 Lattice parameter of the SnO_2 as a function of CuO content at 1,300 °C

3 Results and discussion

Figure 1 illustrates the XRD patterns of the as-prepared SnO_2-based varistor ceramics with different amounts of CuO doping sintered at 1,300 °C for 2 h. There is no any second phase detected in all samples except the SnO_2 rutile phase, which is consistent with the former work [10]. The same trend is observed for samples sintered at 1,200, 1,250, and 1,350 °C. All dopants introduced to the SnO_2 matrix form a stable solid solution according to Eqs. (1), (2), (3) and (4).

$$Co_2O_3 \overset{SnO_2}{\rightarrow} 2Co'_{Sn} + 2V_O^{\bullet\bullet} + 2O_O^x \quad (1)$$

$$2Nb_2O_5 \overset{SnO_2}{\rightarrow} 4Nb_{Sn}^{\bullet} + V_{Sn}'''' + 10O_O^x \quad (2)$$

$$Cr_2O_3 \overset{SnO_2}{\rightarrow} 2Cr'_{Sn} + V_O^{\bullet\bullet} + 3O_O^x \quad (3)$$

$$CuO \overset{SnO_2}{\rightarrow} Cu''_{Sn} + V_O^{\bullet\bullet} + O_O^x \quad (4)$$

The XRD patterns between the 2θ = 26–27° of the sintered products contained different amount of CuO are shown in Fig. 2. It is important to note that the peaks of the SnO_2 diffraction peaks shift towards lower angles with

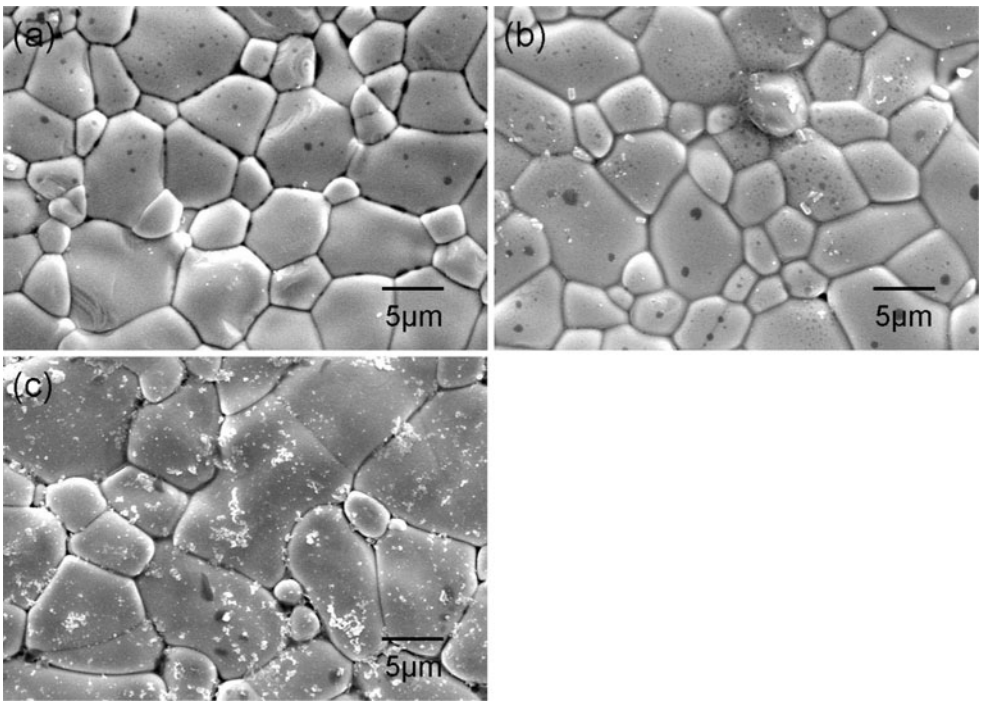

Fig. 4 SEM analysis of SnO_2 varistor ceramics doped with various amount of CuO sintered at 1,300 °C: **a** without CuO; **b** 0.2 mol % CuO; **c** 0.6 mol % CuO

Table 1 Characteristics of the samples doped with different contents of CuO

CuO (mol %)	α	E_B (V/mm)	I_L (μA/cm^2)[a]	Grain size (μm)	Relative density (%)[b]	Shrinkage rate (%)
0.0	25	356	11	4.6	94.9	14.9
0.1	28	343	8	4.7	95.1	15.0
0.2	31	320	2	5.0	95.3	15.1
0.4	29	274	7	5.8	95.2	15.1
0.6	26	248	10	6.2	95.1	15.0

[a] I_L is measured at 0.75 V_{1mA}

[b] Theoretical density of SnO_2 is 6.95 g/cm^3

increasing of CuO content, indicating that the lattice parameter of the as-sintered SnO_2 increases with increasing of CuO content. This is attributable to the solid solution formation between SnO_2 and CuO. The ionic crystal radii of Sn^{4+} and Cu^{2+} are 0.69 and 0.73 Å, respectively. Consequently, one can conclude that the Sn site of SnO_2 lattice could be easily substituted by Cu to form substitutional limited solid solutions. The lattice parameters of the as-sintered $Sn_{1-x}Cu_xO$ samples as a function of CuO content are shown in Fig. 3. It could be observed that both a- and c-axis of the SnO_2 increase as the amount of CuO increases from 0 to 0.6 mol %. Especially, the a-axis decreases more evidently from 4.7179 to 4.7778 Å by 1.26 %, which is obeyed the generally known Vegard's law.

The effect of CuO concentration on the microstructure of the samples is shown in Fig. 4. It reveals that the surfaces of all as fabricated products possess a plain texture with the expected clear grain boundary for ceramic materials. The grain clearance of the samples with 0.2 mol % CuO added is much smaller than those in the samples without CuO and with 0.6 mol % CuO addition. The grain distribution of the samples with 0.2 mol % CuO is also the most homogeneous. The SnO_2 grain size gently increases from 4.6 to 5.0 with the increasing amount of the CuO content from 0 to 0.2 mol %. But it increases evidently from 5.0 to 6.2 with increasing amount of CuO content from 0.2 to 0.6 mol %. It is indicated that few amount of CuO addition mainly improves the density (shown in Table 1) and uniform dispersion of the microstructure of the resultant samples. However, an excess of CuO addition promotes grain growth obviously. That is because CuO will melt at high temperature. It is the liquid CuO at the grain boundary that proved the uniform distribution of dopant and density of the SnO_2 samples. The SnO_2 grain size increases with the overmuch addition of CuO because the substitution of Cu^{2+} for Sn^{4+} increases the activity of SnO_2 by means of distortion of the

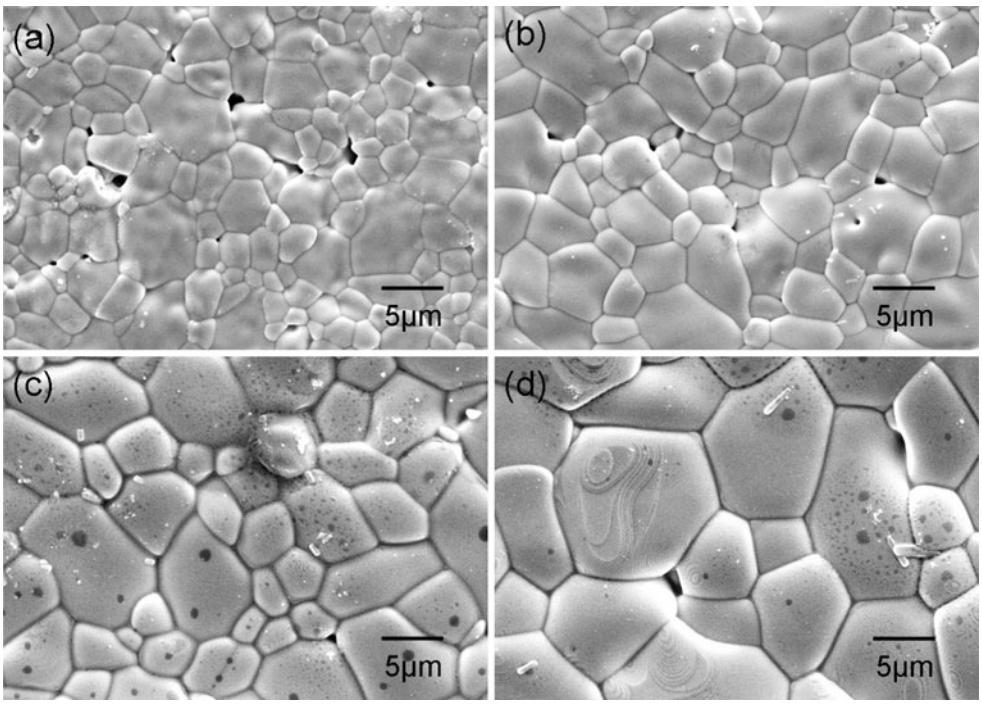

Fig. 5 SEM analysis of SnO_2 varistor ceramics at different temperatures doped with 0.2 mol % of CuO: **a** 1,200 °C; **b** 1,250 °C; **c** 1,300 °C; **d** 1,350 °C

Table 2 Characteristics of the samples doped with 0.2 mol % CuO sintered at different temperatures

Sintering temperature (°C)	α	E_B (V/mm)	I_L (μA/cm^2)[a]	Grain size (μm)	Relative density (%)[b]	Shrinkage rate (%)
1,200	24	664	22	2.8	94.2	14.4
1,250	27	430	16	4.3	94.8	14.8
1,300	31	320	2	5.0	95.3	15.1
1,350	28	253	7	8.4	95.2	15.1

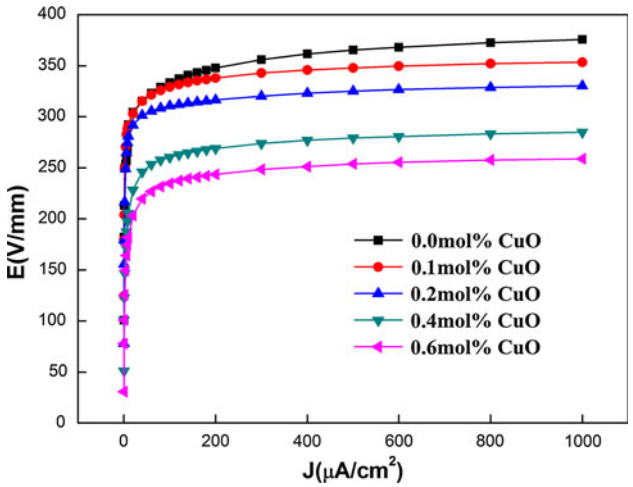

Fig. 6 *I–V* character of the samples doped with different contents of CuO sintered at 1,300 °C

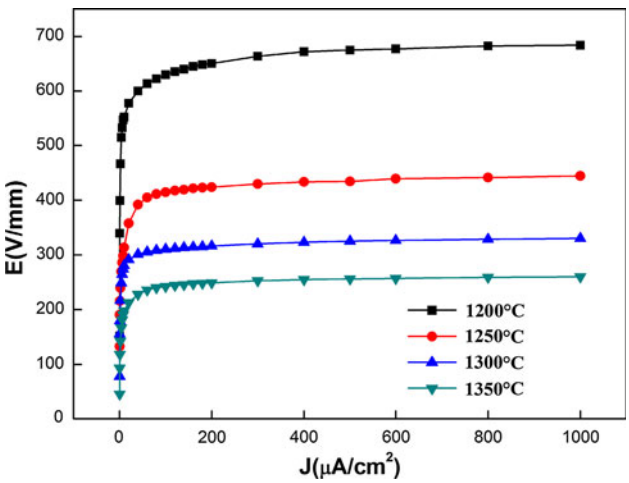

Fig. 7 *I–V* character of the 0.2 mol % CuO added samples sintered at different temperatures

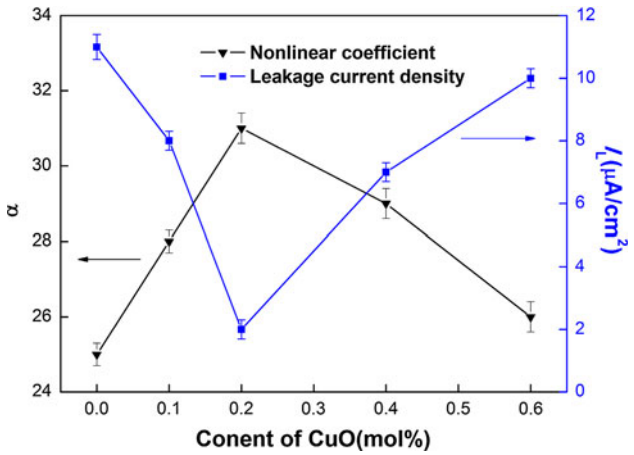

Fig. 8 Nonlinear coefficient and leakage current density of the samples doped with different contents of CuO sintered at 1,300 °C

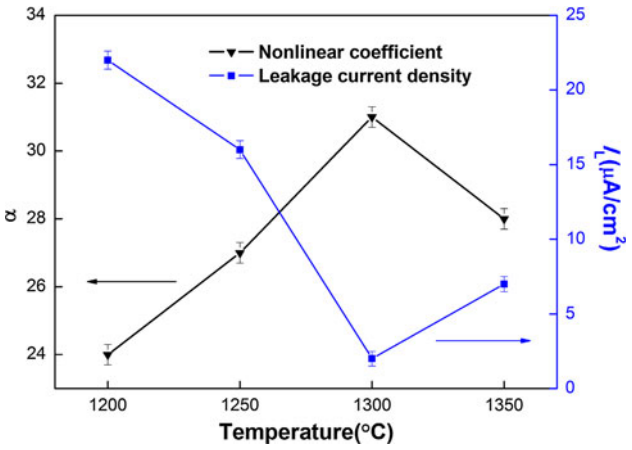

Fig. 9 Nonlinear coefficient and leakage current of the 0.2 mol % CuO added samples sintered at different temperatures

SnO_2 lattice, as discussed in the XRD test. In addition, as seen in the Fig. 5, when the sintering temperature increases to 1,300 °C, the structure is very dense and the grain boundary is very clear, which implies that the SnO_2 grains are well crystallized with good integrality. The grain size grows from 2.8 to 5.0 with an average value. The sintered density of the samples increased from 6.55 to 6.62 g/cm^3 corresponding to 94.2–95.3 % of the theoretical density (TD) (pure SnO_2, TD = 6.95 g/cm^3) when the sintering temperature increases from 1,200 to 1,300 °C. However, the sintered density has little decrease when the sintering temperature up to 1,350 °C, it attributed to the volatility of the liquid at high temperatures. The details are shown in Table 2.

The electrical characteristics of the as fabricated SnO_2-based varistors as a function of CuO concentration sintered at 1,300 °C are plotted in Fig. 6. All the samples have excellent I–V curves in the figures. The breakdown electrical filed decreases from 356 to 248 V/mm with increasing CuO concentration from 0 to 0.6 mol %, which can be explained according to the Eq. (5):

$$E_B = nV_{gb} \tag{5}$$

where n is the average grain number per unit length, V_{gb}, about 2.2–3 V [21], is the breakdown voltage of a grain boundary. As shown in Fig. 4, the average grain size of the sintered samples increases with the increase of the CuO concentration, as a result, the breakdown electrical filed, E_B, decreases. And the breakdown electrical filed decreases from 664 to 253 V/mm with increasing sintering temperature from 1,200 to 1,350 °C, as shown in Fig. 7.

Figure 8 shows that the nonlinear coefficient and leakage current density of the samples with different CuO concentration sintered at 1,300 °C. The nonlinear coefficient has a peak value of 31 when added 0.2 mol % CuO. As the CuO concentration increases above 0.2 mol %, the nonlinear coefficient decreases. According to the previous work [22], the decreasing nonlinear coefficient might be associated to the reduction of the effective grain boundary. On the contrary, The leakage current density decreases firstly with the CuO concentration increasing from 0 to 0.2 mol %, and then increases gradually with the CuO concentration further increasing from 0.2 to 0.6 mol %. As shown in Fig. 4, the high density and uniform microstructure result in lowing the leakage current density of the 0.2 mol % CuO doped SnO_2 samples.

Figure 9 shows the nonlinear coefficient and leakage current density of the 0.2 mol % CuO added samples sintered at different temperatures. The nonlinear of the obtained samples is better than that at any other sintering temperature. Meanwhile, the sample sintered at 1,300 °C presents a lowest leakage current density value of 2 μA/cm^2. As shown in Fig. 5, when the samples with 0.2 mol % CuO addition are sintered at, the product possesses the highest dense and most homogeneous microstructure, which lead to a low leakage current density. Based above results, it can be sure that the 0.2 mol % CuO is the optimum concentration, and 1,300 °C is a appropriate temperature for synthesis of the SnO_2 based varistors.

4 Conclusions

The effect of CuO addition on the microstructure and electrical properties of SnO_2 varistors were studied in detail at different sintering temperatures. The breakdown electrical filed of the SnO_2 varistors decreases with increasing CuO content. While the nonlinear coefficient possesses a peak value of 31 and the leakage current density has the minimum value of 2 μA/cm^2 at 0.2 mol % CuO sintered at 1,300 °C. Hence, the 0.2 mol % is the optimum CuO content for SnO_2 varistors, and 1,300 °C is the best sintering temperature for this system.

Acknowledgments This work was supported by the Scientific and technological project of Wenzhou (H20100079, H20100087), Special project of Shaanxi provincial education department (11JK0810) and the Graduate Innovation Fund of Shaanxi University of Science and Technology.

References

1. S.A. Pianaro, P.R. Bueno, E. Longo, J.A. Varela, J. Mater. Sci. Lett. **14**, 692 (1995)
2. J.A. Cerri, E.R. Leite, D. Gouvea, E. Longo, J.A. Varela, J. Am. Ceram. Soc. **79**, 799 (1996)
3. R. Metz, D. Koumeir, J. Morel, J. Pansiot, J. Eur. Ceram. Soc. **28**, 829 (2008)
4. M.A. Ramirez, J.F. Fernandez, M. De la Rubia, J. De Frutos, P.R. Bueno, E. Longo, J.A. Varela, J. Mater. Sci. Mater. Electron **20**, 49 (2009)
5. L. Perazolli, A.Z. Simoes, U. Coleto Jr, J.A. Varela, Meter. Lett. **59**, 1859 (2005)
6. G. Brankovic, Z. Brankovic, M.R. Davolos, M. Cilense, J.A. Varela, Mater. Charact. **52**, 243 (2004)
7. W.K. Bacelar, P.R. Bueno, E.R. Leite, E. Longo, J.A. Varela, J. Eur. Ceram. Soc. **26**, 1221 (2006)
8. R. Metz, D. Koumeir, J. Morel, J. Pansiot, J. Eur. Ceram. Soc. **28**, 829 (2008)
9. M.O. Orlandi, M.R.D. Bomio, E. Longo, P.R. Bueno, J. Appl. Phys. **96**, 3811 (2004)
10. A.V. Gaponov, A.B. Glot, J. Mater. Sci. Mater. Electron **21**, 331 (2010)
11. F.M. Filho, A.Z. Simoes, A. Ries, E.C. Souza, L. Perazolli, M. Cilense, E. Longo, J.A. Varela, Ceram. Int. **31**, 399 (2005)
12. W.K. Bacelar, P.R. Bueno, E.R. Leite, E. Longo, J.A. Varela, J. Eur. Ceram. Soc. **26**, 1221 (2006)
13. A. Mosquera, J.E.R. Paez, J.A. Varela, P.R. Bueno, J. Eur. Ceram. Soc. **27**, 3893 (2007)
14. M.R.C. Stantos, V.C. Sousa, M.M. Oliveira, F.R. Sensato, W.K. Bacelar, J.W. Gomes, Mat. Chem. Phys. **90**, 1 (2005)
15. G. Brankovic, Z. Brankovic, J.A. Varela, J. Eur. Ceram. Soc. **25**, 3011 (2005)
16. P.A. Santos, S. Maruchin, G.F. Menegoto, A.J. Zara, S.A. Pianaro, Meter. Lett. **60**, 1554 (2006)
17. M.L. Moreira, S.A. Pianaro, A.V.C. Andrade, A.J. Zara, Mater. Charact. **57**, 193 (2006)
18. W.X. Wang, J.F. Wang, H.C. Chen, W.B. Su, G.Z. Zang, Mater. Sci. Eng. B **99**, 457 (2003)
19. C.M. Wang, J.F. Wang, H.C. Chen, W.B. Su, G.Z. Zang, P. Qi, M.L. Zhao, Mater. Sci. Eng. B **116**, 54 (2005)
20. M.I. Mendelson, J. Am. Ceram. Soc. **52**, 443 (1969)
21. E.R. Leite, A.M. Nascimento, P.R. Bueno, J. Mater. Sci. Mater. Electron **10**, 321 (1999)
22. J.S. Vasconcelos, N.S. Vasconcelos, M.O. Orlandi, P.R. Bueno, Appl. Phys. Lett. **89**, 152102 (2006)